CHAPTER

THREE

The Simple Model

Two models were written for the natural convection heat exchanger water loop, one using Fraser's experimental curves, the simple model, and one using correlations found in the literature, the detailed model. This chapter focuses on the model using Fraser's experimental curves.

The simple model can be used to simulate any geometric configuration of sidearm NCHE as long as there are provided experimental curves of shear pressure loss and modified effectiveness. However difficult experiments must be run in order to construct these curves. (See Fraser (1992) for a detailed description of the experimental setup.) The simple model is useful in determining what factors in the hot water system, with the exception of the heat exchanger, affect system

performance. Both the simple and detailed models can be used as tools with which to compare the performance of a natural convection system with a standard pumped system.

3.1 General Considerations

Equations are available for finding static and shear pressure drops from flow rates, for finding heat transfer in heat exchangers, and for determining the flow rate from total pressure heads. Several of these processes depend upon one another. Figure 3.1.2 illustrates the interrelationships for the water loop only. For example, to find the heat transfer rate in the heat exchanger, Q_{HX}, the inlet temperatures and flow rates of glycol and water must be known. The heat transfer rate in turn determines the outlet temperatures from the heat exchanger, which affect the tank temperature. These temperatures determine the densities and viscosities of the water around the loop, which in turn are used to calculate the static and shear pressure heads . The water flow rate is determined from the pressure equations. Each of the variables described is dependent upon the other variables in the loop. The modeling of each of the individual processes is simple. However, development of a model that combines these is somewhat difficult due to these complex interrelationships.

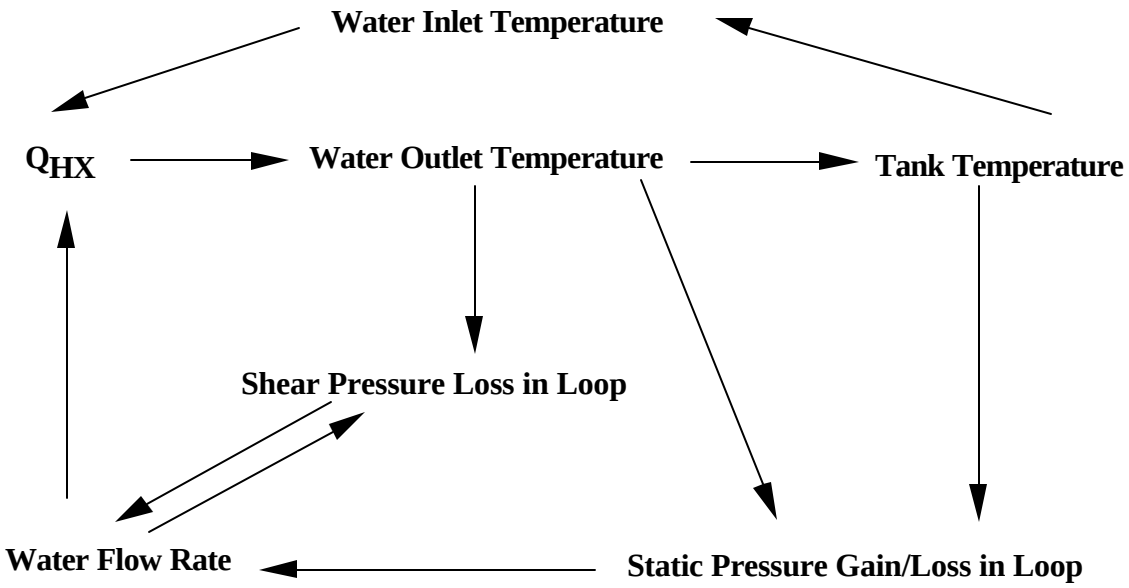

Figure 3.1.2 The complex interrelationship of variables in the natural convection water loop. The arrows represent information flow.

3.2 Pressure Drop Calculations

At any instant of time in any fluid loop, the total pressure difference around the loop must equal zero, that is,

$$\oint \Delta P = 0 \qquad (3.2.1)$$

where

$$\oint \Delta P = \Delta P_{NCHE} + \Delta P_{Tank} + \Delta P_{pipes} \qquad (3.2.2)$$

and where DP_{NCHE}, DP_{Tank}, and DP_{pipes} represent the combined static and shear pressure heads in the NCHE, the tank and pipes respectively, as is shown in Figure 3.2.1. Each pressure change term consists of the change in pressure due to static and shear or frictional losses, that is,

$$\Delta P = \Delta P_{st} + \Delta P_{sh} \qquad (3.2.3)$$

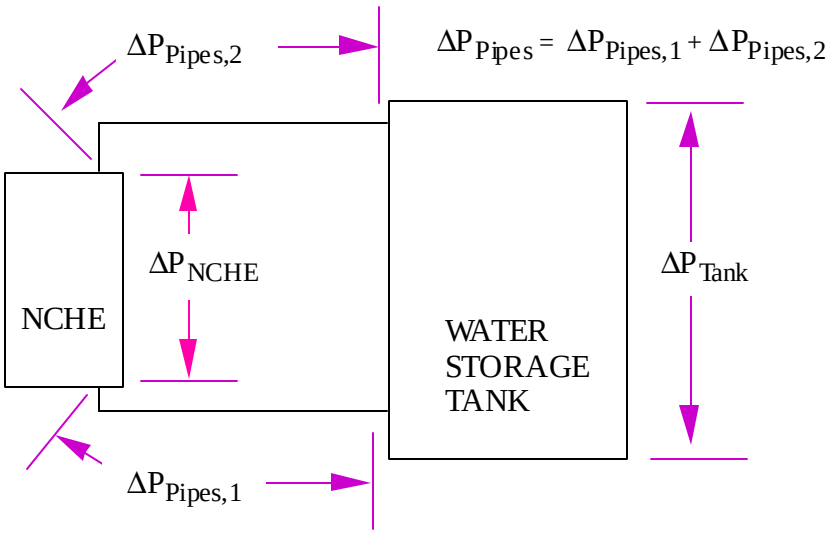

Figure 3.2.1 Summation of pressure drops in the water loop must equal zero.

This requirement then, is used in the following form:

$$\oint \Delta P_{sh} + \oint \Delta P_{st} = 0 \qquad (3.2.4)$$

The following sections outline the procedure used in finding $\oint \Delta P_{st}$ and $\oint \Delta P_{sh}$.

3.2.1 Pressure Drop in Pipes

In order to model the NCHE loop, it is necessary to find the static and shear friction losses around the water loop. The static pressure drop is a function of density, while the shear pressure drops are functions of water flow rate and viscosity. Density and viscosity, in turn, depend upon the temperatures of the fluid. The static pressure drops/gains for each component in the water loop are found using the equation,

$$DP_{st} = \int_{inlet}^{outlet} r\, g\, dz \qquad (3.2.5)$$

where dz is measured from the component inlet to the component outlet. In cases where the inlet is vertically higher than the outlet, dz is considered negative, otherwise dz is assigned a positive value.

Assuming laminar flow the Darcy friction factor is found using the Darcy equation:

$$f_D = \frac{64}{Re_D} \qquad (3.2.6)$$

The shear pressure drops in the pipes connecting the heat exchanger and the tank can then be calculated using equation:

$$\Delta P_{sh} = f_D \frac{L_p}{D_p} \rho \frac{V^2}{2} \qquad (3.2.7)$$

where L_p and D_p are the length and diameter of the pipes, and V is the velocity of fluid in the pipes. Valves, elbows and other fittings are assigned minor loss coefficient, K values, which can be converted into equivalent pipe length values using the following equation:

$$L_e = \frac{K \dot{m} Y}{16 \pi \mu(T)} \qquad (3.2.8)$$

To find the shear pressure drop associated with each fitting, the equivalent length, L_e, can then be inserted into the shear pressure drop equation, Equation 3.2.7. The shear pressure drops attributable to minor losses are then added to the shear losses associated with the pipes.

3.2.2 Pressure Drop in Water Storage Tank

As the water storage tank inlet is above the outlet, Dz is considered negative for the tank as is shown in Figure 3.2.2. The static pressure gain in the water storage tank, like that of the pipes, can be found using the static pressure drop equation, Equation 3.2.5.

Shear pressure drop in the tank can be safely neglected due to the tank's large diameter.

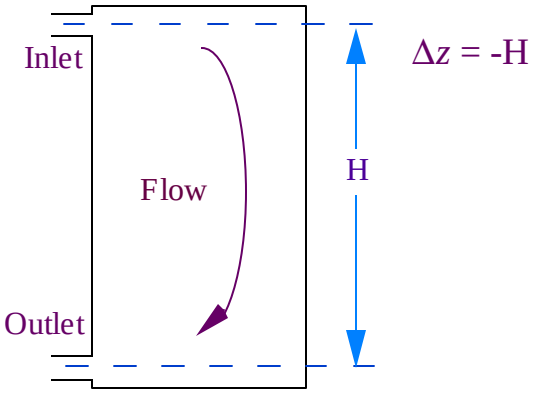

Figure 3.2.2 As the water flow in the water storage tank proceeds from top to bottom, *Dz* is considered negative.

3.2.3 Pressure Drop in NCHE

Static pressure drop in the NCHE was found using Equation 3.2.5. Fraser presented experimental data describing the relationship of shear pressure drop across the heat exchanger as a function solely of water flow rate. It was found that the shear pressure drop was essentially independent of water temperature. Her results are presented in Figure 3.2.3. Data from this curve was placed into data files to be accessed by the simple model which is described in Chapter 5.

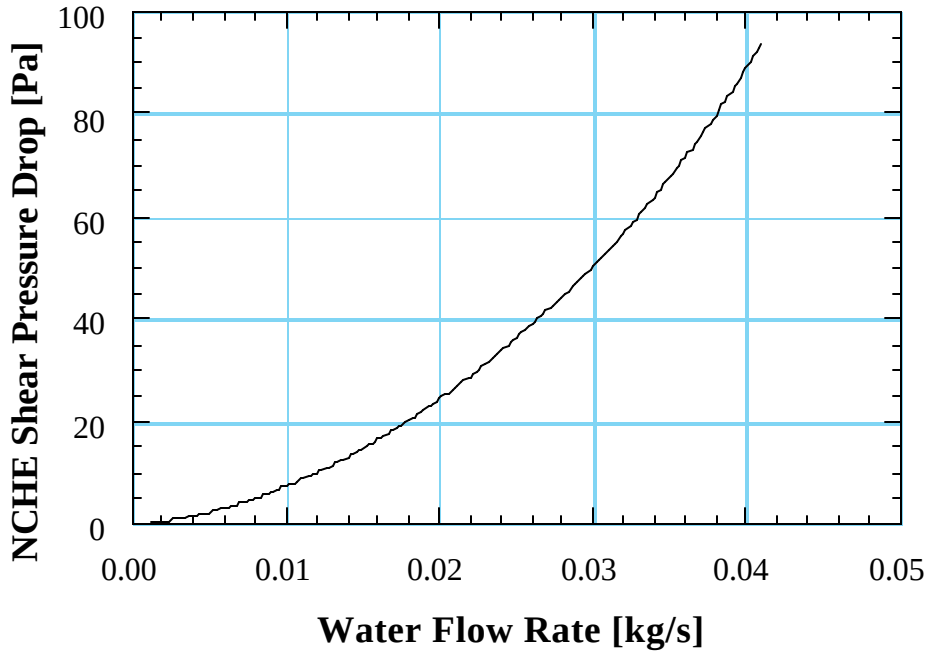

Figure 3.2.3 ΔP_{shear} curve for NCHE adapted from Fraser (1992).

3.3 Heat Transfer Calculations

3.3.1 NCHE Temperature Profile

Assuming perfectly counterflow behavior and constant specific heats, Fraser presents an equation derived from Fraas (1989) for the water side temperature distribution in the NCHE:

$$T(z) = T_{w,i} + \left(\frac{T_{g,o} - T_{w,i}}{\Delta T_g - \Delta T_w} \right) \left[1 - \left(\frac{T_{g,i} - T_{w,o}}{T_{g,o} - T_{w,i}} \right)^{\frac{z}{H}} \right] \qquad (3.3.1)$$

where $T(z)$ = HX temperature at node z ,
$T_{w,i}$ = HX water inlet temperature ,
$T_{w,o}$ = HX water outlet temperature ,
$T_{g,i}$ = HX glycol inlet temperature ,
$T_{g,o}$ = HX glycol outlet temperature ,
DT_g = HX glycol temperature difference ,
DT_w = HX water temperature difference ,
H = HX height ,
and z = height of node .

Average water density in the heat exchanger is found by finding the density at N points in the heat exchanger and integrating using the trapezoidal rule.

3.3.2 Effectiveness-NTU Relationships

One way to find the heat transfer in a counterflow heat exchanger is to use the effectiveness-NTU method, in which effectiveness is the ratio of the amount of energy that is transferred from the hot fluid to the maximum amount of energy that could be transferred:

$$e = \frac{Q_{HX}}{Q_{\max}} = \frac{\left(\dot{m}C_p\right)_g \left(T_{g,i} - T_{g,o}\right)}{\left(\dot{m}C_p\right)_{\min} \left(T_{g,i} - T_{w,i}\right)} = \frac{\left(\dot{m}C_p\right)_w \left(T_{w,o} - T_{w,i}\right)}{\left(\dot{m}C_p\right)_{\min} \left(T_{g,i} - T_{w,i}\right)} \qquad (3.3.2)$$

where e = HX effectiveness ,
Q_{HX} = HX heat transfer rate [W],
$Q_{\max}$ = maximum heat transfer rate [W],
$\left(\dot{m}C_p\right)_g$ = glycol capacitance rate [J / K - s],
$\left(\dot{m}C_p\right)_w$ = water capacitance rate [J / K - s],
and $\left(\dot{m}C_p\right)_{\min}$ = minimum capacitance rate [J / K - s].

The effectiveness is a function of the overall heat exchanger heat transfer coefficient and the fluid capacitance rates, thus for a counterflow heat exchanger (Thomas 1992):

$$\varepsilon = \frac{1-\exp\left[-NTU\left(1-C^*\right)\right]}{1-C^*\exp\left[-NTU\left(1-C^*\right)\right]} \tag{3.3.3}$$

$$\text{where} \quad C^* = \frac{\left(\dot{m}C_p\right)_{\min}}{\left(\dot{m}C_p\right)_{\max}} \tag{3.3.4}$$

$$\textit{and} \qquad NTU = \frac{UA_s}{\left(\dot{m}C_p\right)_{\min}} \tag{3.3.5}$$

$$\textit{if} \quad C^* = 1, \ \varepsilon = \frac{NTU}{1+NTU} \tag{3.3.6}$$

where $\left(\dot{m}C_p\right)_{\max}$ is the maximum capacitance rate, and UA_s is a function of the geometry and heat transfer characteristics of the heat exchanger.

As the specific heats do not vary much with temperature, for a fixed geometry, effectiveness at a constant glycol flow rate can be assumed to be solely a function of the water flow rate.

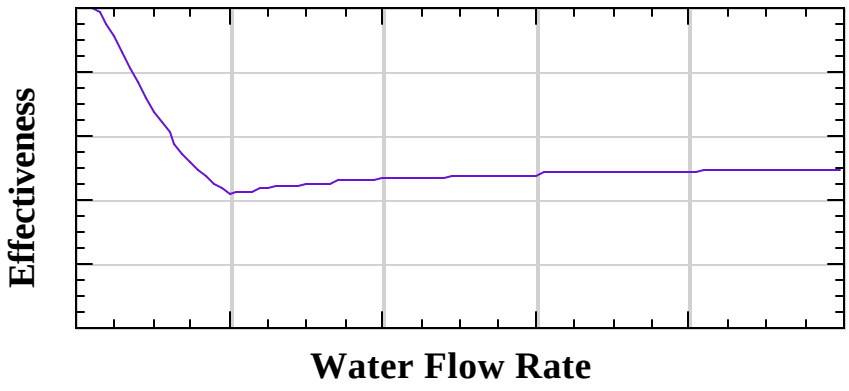

Figure 3.3.1 Effectiveness curve for varying water flow rate. At low water flow rates, the effectiveness does adequately represent the performance of the NCHE.

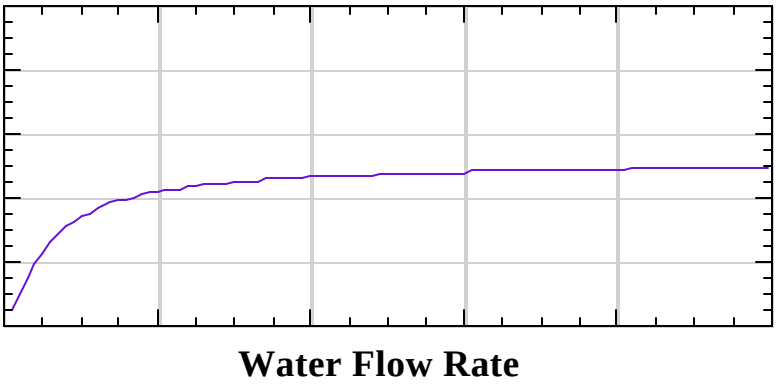

Figure 3.3.2 Modified effectiveness curve for varying water flow rate.

A valid indicator of the performance of a heat exchanger in a SDHW system can be considered to be the degree to which the cold fluid can reduce the temperature of the hot fluid in the heat exchanger to the cold fluid's inlet temperature, which is called effectiveness. Higher water flow rates will allow better heat transfer from the hot fluid to the cold fluid in the heat exchanger. However, at low water flow rates, Figure 3.3.1 reports a higher effectiveness until the cusp in the effectiveness curve, while heat transfer between the fluids, in actuality, is limited by the low water flow rates. Therefore Fraser defined a modified effectiveness as a more appropriate measure of a NCHE's performance. Figure 3.3.2 shows a modified effectiveness curve.

3.3.3 Modified Effectiveness Relationships

Rather than have C^* equal the ratio of the maximum to minimum capacitance rate, Fraser sets C^* equal to the ratio of the glycol to water capacitance rates, that is,

$$C^* = \frac{(\dot{m}C_p)_g}{(\dot{m}C_p)_w} \qquad (3.3.7)$$

$$and \quad NTU = \frac{UA_s}{(\dot{m}C_p)_g} \tag{3.3.8}$$

As is shown in Figure 3.3.2, a typical modified effectiveness versus water flow rate plot is smooth.

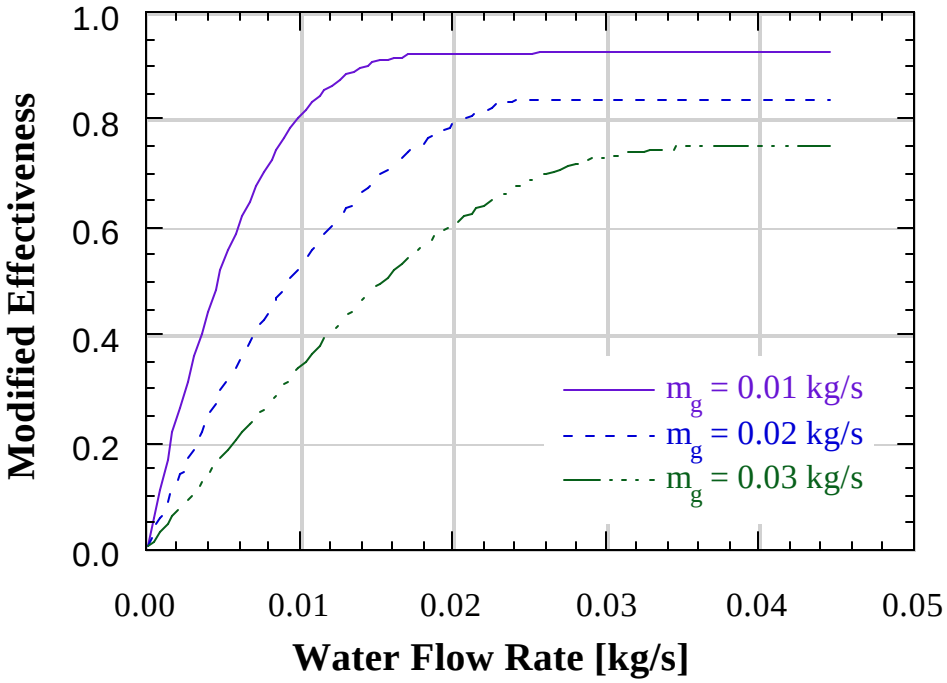

Figure 3.3.3 Fraser's experimental modified effectiveness curves

Through experiment, Fraser constructed modified effectiveness curves that are a function solely of the water and glycol flow rates as is shown in Figure 3.3.3. Data at intervals of 0.005 kg/s were read from the curves, set into data files, and used in an interpolation subroutine in the simple model.

3.3.4 Heat Exchanger Energy Relationships

Assuming a counter flow heat exchanger, and employing modified effectiveness, the heat exchanger energy relationships become:

$$Q_{HX} = (\dot{m}Cp)_w (T_{w,o} - T_{w,i}) \tag{3.3.9}$$

$$Q_{HX} = (\dot{m}Cp)_g \left(T_{g,i} - T_{g,o}\right) \quad (3.3.10)$$

$$Q_{HX} = e'(\dot{m}Cp)_g \left(T_{g,i} - T_{w,i}\right) \quad (3.3.11)$$

where e' represents the modified effectiveness.

3.3.5 Density Correction Term

Fraser measured the pressure drop across a vertically suspended heat exchanger. In order to obtain the shear pressure drop curve for the heat exchanger, she had to subtract the static pressure drop from the measured total pressure drop.

$$\Delta P_{sh} = \Delta P_{exp} - \Delta P_{st} \quad (3.3.12)$$

where ΔP_{exp} is the measured pressure drop. The static pressure drop is a function of the average density in the heat exchanger. Using the counterflow assumption and the associated average water density in the heat exchanger, Fraser determined the shear pressure drop using equation 3.3.12. This procedure produced negative shear pressure drops for low water flow rates, which cannot occur. Assuming the pressure measurements were correct, the average density value of the water must have been incorrect, which meant that the perfectly counterflow temperature distribution did not apply. Therefore Fraser was forced to create a density correction factor.

As outlined in Section 2.3, the water in the heat exchanger is propelled by forced convection. However at low flow rates, natural convection effects within the heat exchanger, itself, become evident. As cold water comes into contact with the hot helices of glycol, the water heats up locally. This water then becomes less dense and rises within the heat exchanger, displacing the cooler water around it. As the water rises in the heat exchanger, mixing occurs, and the average temperature of the water in the heat exchanger becomes warmer than the average temperature found using the

perfectly counterflow assumption and the corresponding temperature distribution presented in Section 3.3.1. In order then to find an average density value for the heat exchanger, Fraser proposed the empirical density correction factor:

$$\bar{\rho}_{HX} = W\bar{\rho}_{cf} + (1-W)\rho_{w,o} \qquad (3.3.13)$$

where $W = \min\left(1, \frac{\dot{m}_w}{0.012}\right)$,

$\bar{r}_{cf}$ = HX average density using counterflow assumption ,

and $r_{w,o}$ = density at HX water outlet .

For flow rates below 0.012 kg/s, the density of the heat exchanger is considered to be a weighted average between the average density in the heat exchanger using the perfectly counterflow assumption, and the density of the outlet water temperature. The density correction term is considered in more detail in Section 3.5.

3.4 Other Considerations

3.4.1 NCHE Water Outlet Temperature as Water Flow Approaches Zero

Figure 3.4.1 illustrates that when the water flow rate approaches zero, the water outlet temperature approaches the glycol inlet temperatures of 50 °C. For a zero water flow rate, according to Equation 3.3.9 the heat transfer rate in the heat exchanger becomes zero. To extract the water outlet temperature from Equation 3.3.9, the energy balance takes the form:

$$T_{w,o} = T_{w,i} + \frac{Q_{HX}}{\left(\dot{m}C_p\right)_w} \qquad (3.4.1)$$

When there is no water flow, Equation 3.4.1 requires division by zero, which cannot happen. To avoid dividing by zero, Equations 3.3.9 and 3.3.11 can be combined to form:

$$T_{w,o} = T_{w,i} + e' \frac{\left(\dot{m} C_p\right)_g}{\left(\dot{m} C_p\right)_w} \left(T_{g,i} - T_{w,i}\right) \qquad (3.4.2)$$

and the limit as the water flow rate approaches zero can then be taken:

$$T_{w,o} = T_{w,i} + \frac{\varepsilon_1'}{\dot{m}_{w,1}} \frac{C_g}{C_{p,w}} \left(T_{g,i} - T_{w,i}\right) \qquad (3.4.3)$$

where $\dot{m}_{w,1}$ and e_1' represent the first flow rate and modified effectiveness values in the data file for a given glycol flow rate. The outlet water temperature using Equation 3.4.3 corresponds to Figure 3.4.1's water outlet temperature of 50.0 °C, as water flow approaches zero.

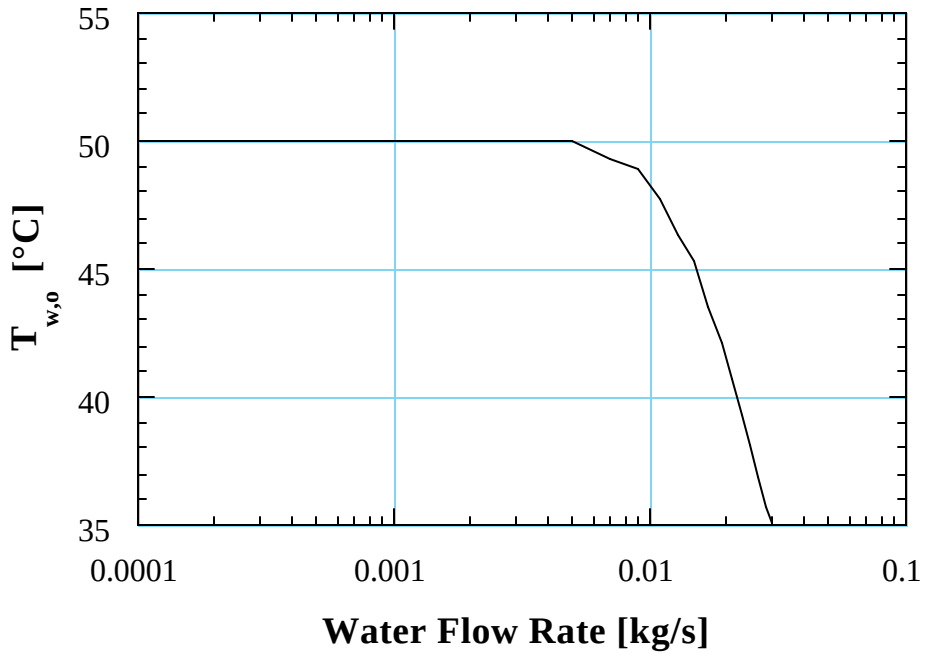

Figure 3.4.1 HX water outlet temperature as water flow rate approaches zero. The water outlet temperature approaches neither the glycol or water inlet temperatures.

3.4.2 Iterating within the Model

The physics behind the simple model have been presented. Figure 3.4.2 lists pseudocode displaying the order of calculation.

1) INPUT: T_w,i, T_g,i, m_g, m_w, DP_tank
2) FIND PROPERTIES: C_p, Density, viscosity
3) FIND CAPACITANCE RATES (based on average HX temps.)
4) FIND EFFECTIVENESS FROM WATER FLOW RATE
5) ENERGY BALANCES: FIND OUTLET TEMPS.
6) NCHE TEMP. DISTRIBUTION: FIND AVE HX DENSITY, TEMPS.
7) FIND PROPERTIES AGAIN: C_p, Density, viscosity
8) FIND DP_shear, DP_static
9) OUTPUT: T_w,o, T_g,o, DP_shear, DP_static

Figure 3.4.2 Pseudocode of the simple model calculation order.

For inputs of T_{wi}, T_{gi}, m_w, and ΔP_{tank}, the water capacitance rate is a function of the average water temperature in the heat exchanger:

$$C_w = f\left(\overline{T}_{HX}\right) \tag{3.4.4}$$

and the average temperature in the heat exchanger is a function of the water outlet temperature and the water capacitance rate,

$$\overline{T}_{HX} = f\left(C_w, T_{w,o}\right) \tag{3.4.5}$$

The water outlet temperature is a function of the water capacitance rate,

$$T_{w,o} = f\left(C_w\right) \tag{3.4.6}$$

The three variables, C_w, $\overline{T}_{HX}$, $T_{w,o}$, all depend upon one another. As the capacitance rate, found in step 3 in Figure 3.4.2, corresponds to the average temperature in the heat exchanger, which is found in step 6, the capacitance rate found in one iteration will correspond to the average heat exchanger temperature of the last iteration or time step. Therefore it is necessary to iterate within

the model, until the output temperatures converge upon a value. Until the average heat exchanger temperatures and the capacitance rates converge, the outlet temperatures and pressure drops will not be accurate.

3.4.3 Questions Concerning Fraser's Density Correction Factor

Fraser had two uses for the density correction factor (DCF): first, in order to find more accurate average water densities in the heat exchanger, and second, in order to determine the shear pressure drop curve (as was presented in Section 3.3.5).

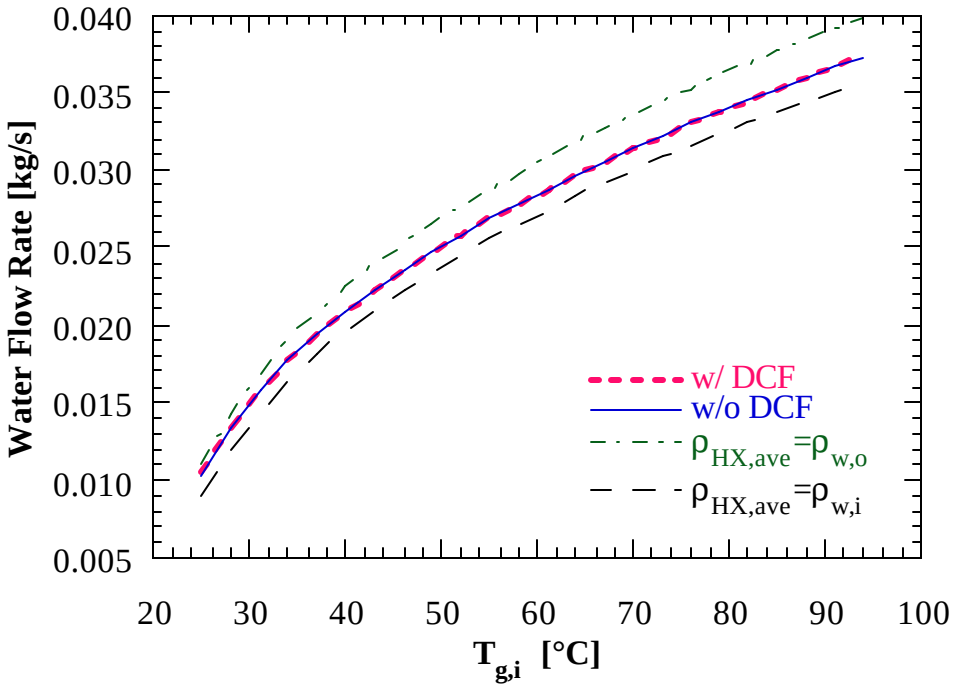

Figure 3.4.3 Effect of Fraser's density correction factor (DCF) on water flow rate. Also presented are water flow rates for the hypothetical cases of HX inlet and outlet densities used to represent average HX densities.

The use of the DCF was found to have little effect upon simulation results. Consider the case in Figures 3.4.3-4. A steady state model, run both with and without the DCF, shows how little effect the DCF had. Although the DCF's effect was small, the average density values used for the heat exchanger is indeed significant. When the water inlet density is assumed to be the average density in the heat exchanger, the water flow rate decreases substantially, and when the outlet density is used the water flow rate increases substantially. However, it is interesting to note that the heat transfer in the heat exchanger is essentially the same for both cases.

Simulations were carried out for April in Madison for a fixed set of conditions, both with and without the DCF. The presence of the DCF in the model changes the solar fraction less than 0.5%. Simulations were also executed assuming the heat exchanger average density is the

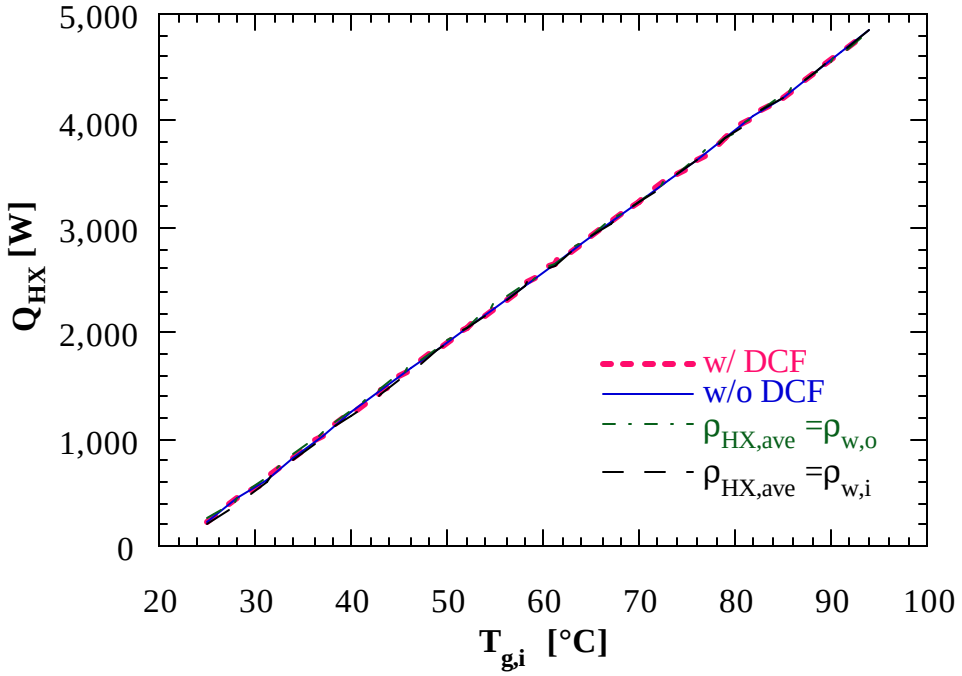

Figure 3.4.4 Effect of Fraser's DCF on heat transfer in HX. Also presented is heat transfer for the hypothetical cases of HX inlet and outlet densities used to represent average HX densities.

same as the water inlet and outlet densities as well, as in the steady state model. Although the heat transfer in the steady state model was essentially the same for different flow rates, in transient simulations, this small density variation has a substantial effect. Table 3.4.1 shows a 5.79% difference in solar fraction.

Table 3.4.1 The Transient Effect of Density Correction Factor

Mode	Solar Fraction
w/ DCF	0.574
w/o DCF	0.572
% difference	0.45 %
$\rho_{ave,HX}=\rho_{w,i}$	0.549
$\rho_{ave,HX}=\rho_{w,o}$	0.581
% difference	5.79 %

One can conclude then, that the average density value chosen for the heat exchanger is of importance in the model, and needs to be chosen carefully, but the use of the density correction factor has little effect on simulation results.

3.4.4 Measuring Shear Pressure Drop in the NCHE

In finding the shear pressure drop in the NCHE, Fraser used both no-heating and heating tests. In both tests water was pumped in the water loop and a flow control valve was used to vary the water flow rate. In the no-heating tests, water was pumped through the NCHE, such that the water inlet and outlet temperatures remained the same. No energy was transferred to the water. Pressure was measured at the water inlet and outlet of the heat exchanger. For the heating tests, Fraser heated the glycol in the glycol loop and performed the same procedure, to establish that the pressure drop was not related to temperature. By doing so, Fraser measured the total pressure drop in the

NCHE. The shear pressure drop was found by subtracting the static pressure drop in the heat exchanger from the measured total NCHE pressure drop, as was described in Section 3.3.5. The static pressure drop in the heat exchanger is determined using an average heat exchanger density which itself is determined from the temperature distribution which cannot be known, only assumed. Consequently the shear pressure drop curve is influenced by the counterflow temperature distribution assumption, and Fraser's density correction factor, and may not be entirely correct.

A better way to measure the shear pressure drop could be to put the NCHE on its side and then to measure the pressure difference (Davidson 1994). Better shear pressure drop curves could then be found, as the assumptions regarding temperature distribution would no longer affect the curves. As well, this is a simpler method. These improved measurements should not affect the model presented herein. Better pressure drop data, when it becomes available, can be inserted into data files and accessed by the program.

In conclusion, Fraser's density factor can be done away with in its entirety, if shear pressure drop tests for the NCHE were done with the heat exchanger lying horizontally. As the density correction has negligible effect on simulation results, it need not be inserted into the model.

3.5 Comparison of Simple Model to Fraser's Experimental Results

In order to validate the simple model, TRNSYS simulation results were checked against Fraser's experimental and simulation results for both the steady state and transient cases, which are described in Chapter 1. Figures 3.5.1-2 present a comparison of simulation results and experimental data for the steady state condition. It is obvious, that although the simulation results for

the simple model and Fraser's model are close, the experimental data and the models do not agree well.

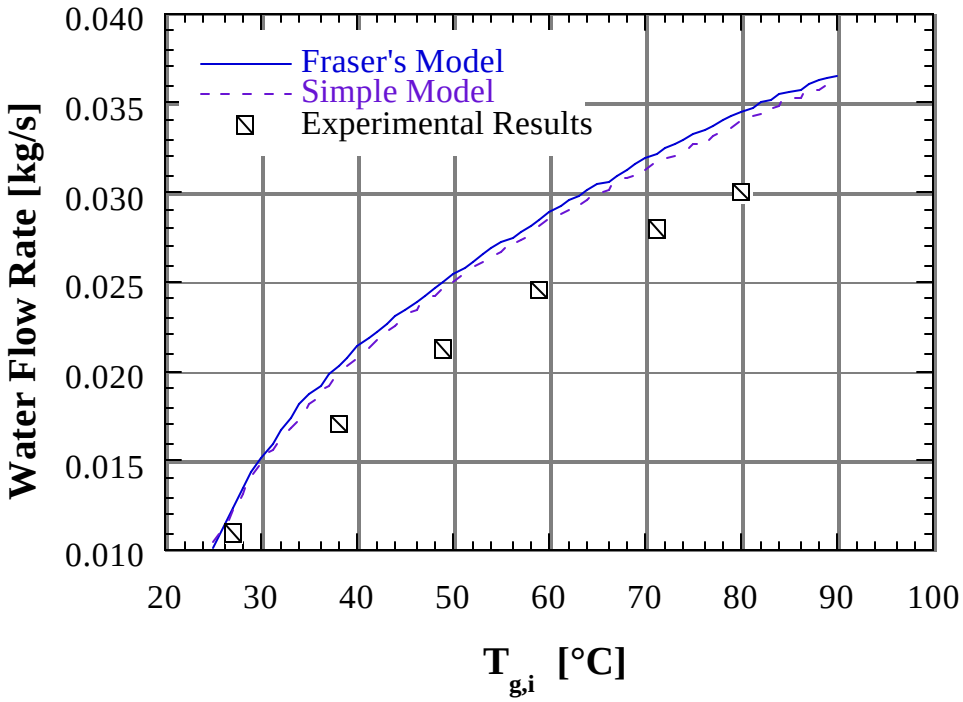

Figure 3.5.1 Comparison of simple model to Fraser's simulation and experimental results: water flow rates for the steady state condition.

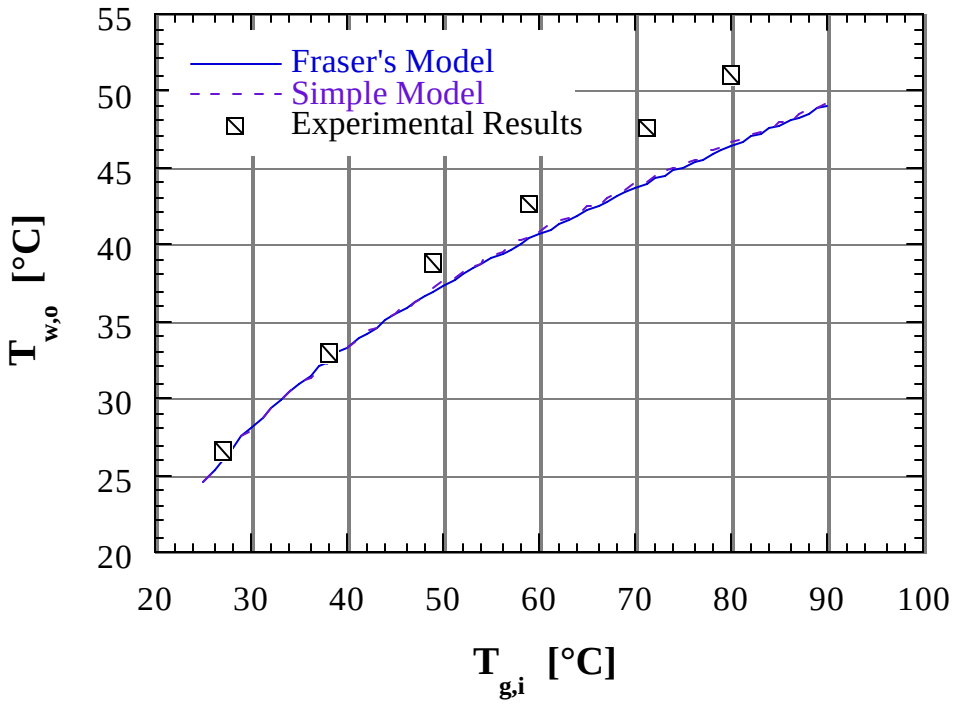

Figure 3.5.2 Comparison of simple model to Fraser's simulation and experimental results: water outlet temperatures for the steady state condition.

For the steady state tests, Fraser compared the experimental modified effectiveness (which was calculated from temperature measurements) and the measured shear pressure drop across the heat exchanger to the curves she had originally constructed and inserted into the model (which are presented in Figures 3.2.3 and 3.3.3). As the data points matched the modified effectiveness and shear pressure drop curves closely, Fraser decided that the discrepancy, other than experimental uncertainly, must be in the model of the pressure drop around the rest of the water loop. Fraser concluded that this disparity was due mostly to a poor accounting for shear minor loss conditions in the water loop. Fraser's test rig, onto which the heat exchanger was attached, included 11 piping connections in the water loop, as well as a 360° bend. As is explained in Section 4.2.1, minor loss coefficients found in tables correspond to turbulent, not laminar, flow conditions, whereas the flow experienced in the water loop is laminar. It is likely the minor loss coefficients Fraser used in modeling the water loop come from such tables. As well, the shear pressure losses of a series of

ells, flow entrance and exit conditions, and valves in close proximity tend to compound shear pressure losses.

Fraser found that the model is very sensitive to minor loss coefficient inputs. As would be expected, for the smallest diameter piping in the loop (the NCHE outlet piping), changes in minor loss coefficients had the greatest effect upon simulation results. Increasing the minor loss coefficient of this smallest diameter pipe by 5 (which increases the total minor loss coefficients by 40%) led to a good simulation correspondence with experimental data, as is shown in Figure 3.5.3-4.

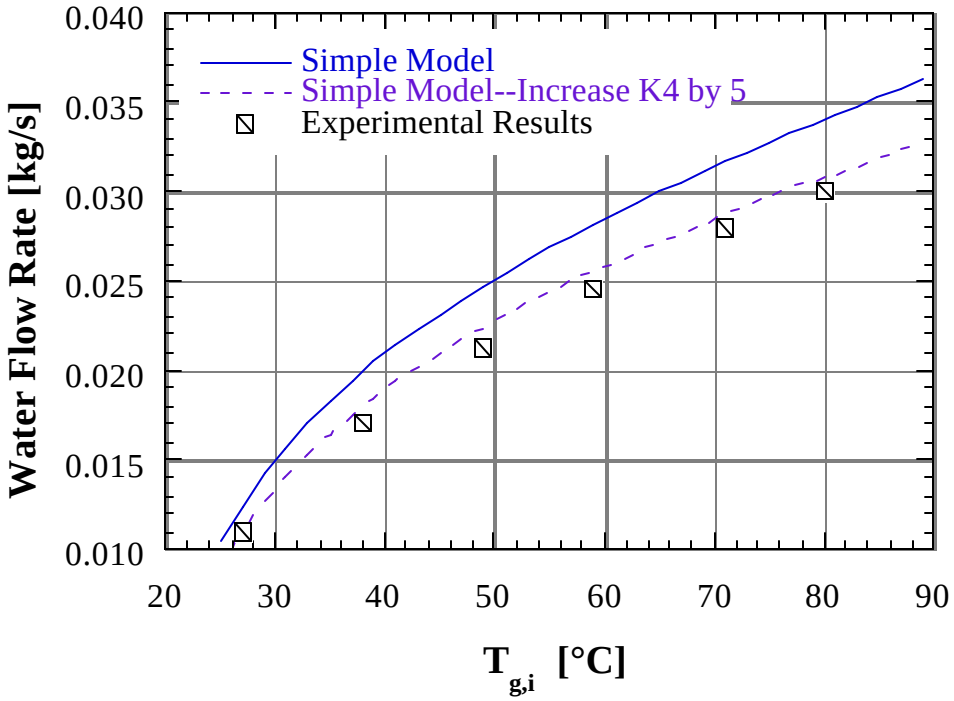

Figure 3.5.3 An increase in the minor loss coefficient corresponding to the smallest diameter pipe in the water loop leads to a good correspondence between the simple model and experimental results: steady state water flow rate as a function of glycol inlet temperature.

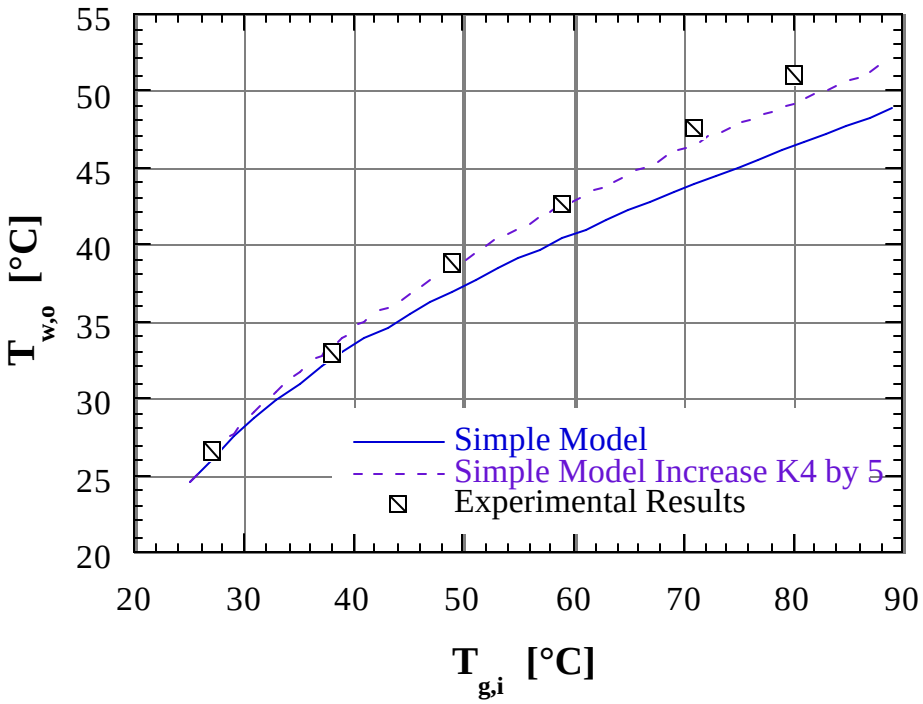

Figure 3.5.4 Steady state water outlet temperature as a function of glycol inlet temperature for an increased minor loss coefficient..

In any case, the models and experimental data differ by approximately 13.5% for water flow rate, and about 8% for water outlet temperature. As is shown in Figure 3.5.5, although the simulation results and experimental data for water flow rate and the water outlet temperature do not compare well, the heat transfer rate does.

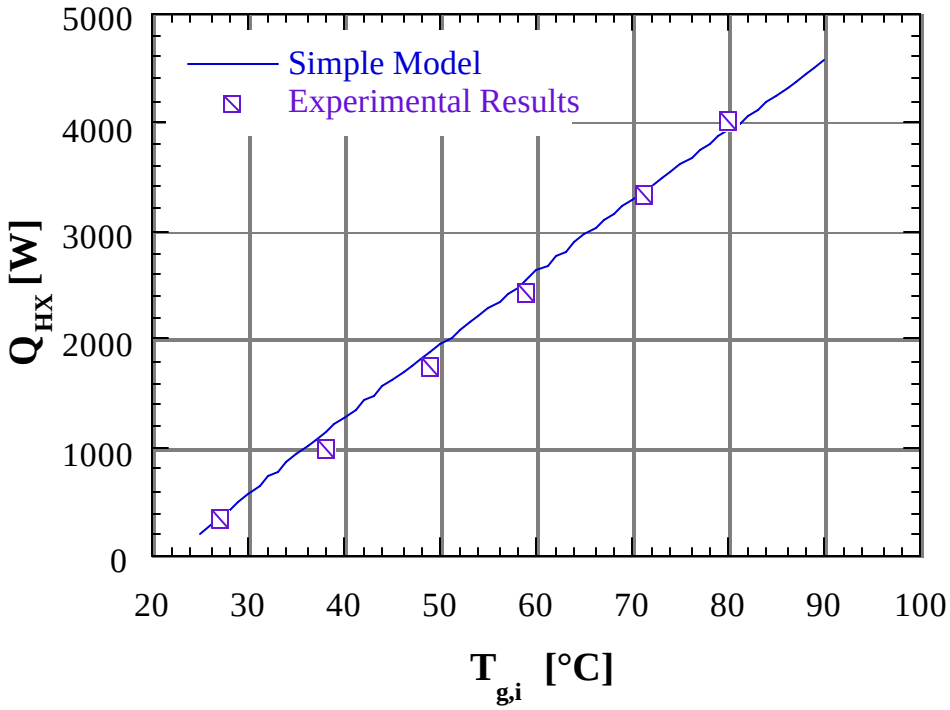

Figure 3.5.5 Comparison of simple model to Fraser's experimental results: heat transfer rate in the heat exchanger for steady state condition.

Figures 3.5.6-7 present a comparison of simulation results for the transient case, as defined in Chapter 1. The same trends are evident in the transient case, as were in the steady state case. The model overpredicts the water flow rate and underpredicts the water outlet temperature.

In sum, it is believed that the model works well. However it is very sensitive to the minor loss coefficients that serve as inputs to the model. Care must be taken when using the model to accurately specify the minor loss coefficients for the water loop.

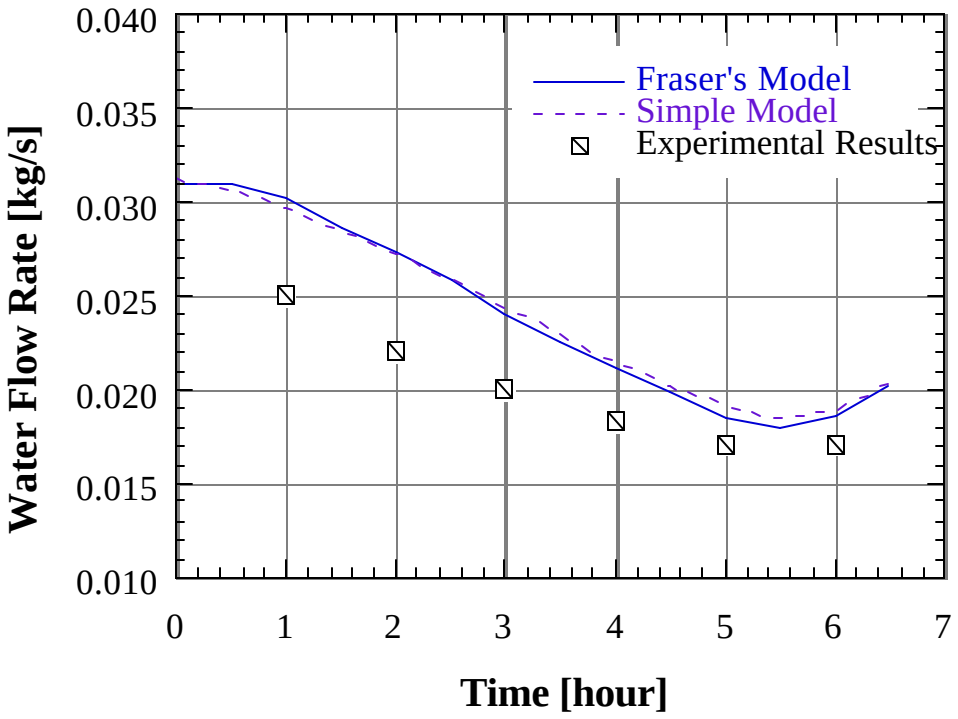

Figure 3.5.6 Comparison of simple model to Fraser's simulation and experimental results: water flow rates for the transient condition.

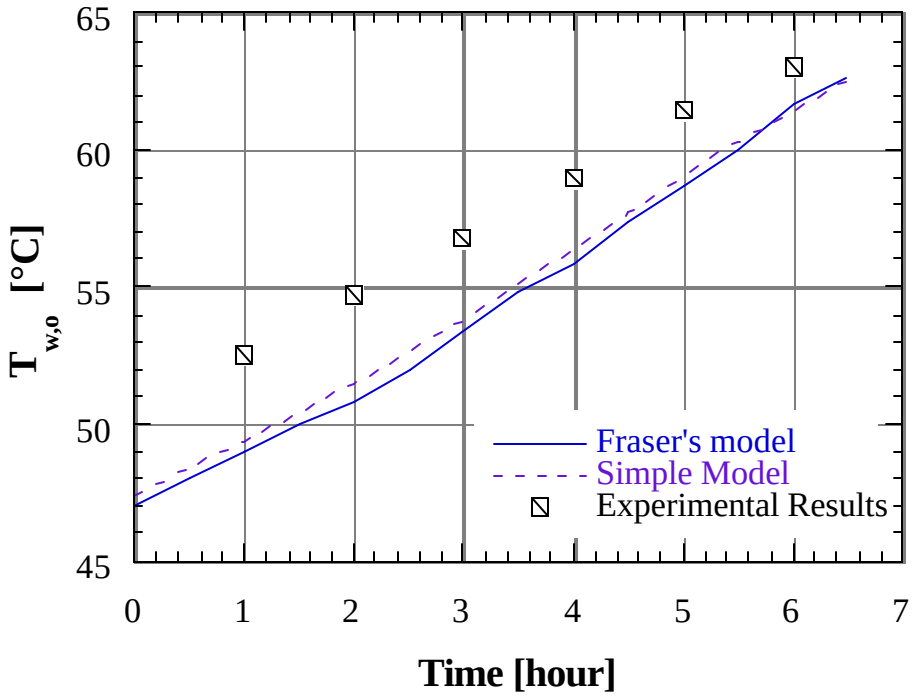

Figure 3.5.7 Comparison of simple model to Fraser's simulation and experimental results: water outlet temperatures for the transient condition.